Journal of Bio-Molecule Research and Engineering
Vol. 1 | No. 1| 73 – 88 | 2022
e-ISSN: 2962-343X
http://www.e-journal.unair.ac.id/biome

Semi-empirical Study of Acetic Acid Esterification and Methyl Ester Transesterification Reactions with Nafion Catalyst using PM7 Level of Theory

Fariz R. Alfian[1*], Farly Y. Faiq[1], Rafli Rizaldy[1], and Kautsar Ul Haq[1]
[1]Department of Chemistry, Airlangga University, 60115, Indonesia.
*Corresponding author. Tel/Fax: +62 87742235146
E-mail address: fariz.rizky.alfian-2020@fst.unair.ac.id

ARTICLE INFO
Article history
Received 18th Oct 2022
Accepted 9th Dec 2022
Keywords:
catalyst
esterification
transesterification
Semi-empirical
PM7

ABSTRACT

Nafion, as a highly acidic catalyst, is appropriate for application in both esterification and transesterification reactions. Nevertheless, its computational efficacy hasn't been explored yet. A semi-empirical approach employing the PM7 theory was utilized to determine the configurations of reactants, transition states, intermediates, and products, along with the energetics of the reactions. The findings indicate that, with Nafion catalysts, a 6-ring complex is formed in both reactions, and the rate-determining step occurs at the initial activation energy. Additionally, a quantum leap in reaction kinetics was observed in the presence of the Nafion catalyst, leading to an accelerated reaction rate.

1. Introduction

In the modern era, various alternative energy sources have emerged as viable options to replace fossil fuels, with biodiesel being one such alternative. Biodiesel is characterized as a diesel fuel variant consisting of long-chain fatty acid esters derived from vegetable oils or animal fats, offering a non-toxic and biodegradable alternative energy solution [1]. In Indonesia, palm oil serves as the primary raw material for biodiesel production, owing to its abundant availability in the country. Nevertheless, challenges arise concerning the competition for palm oil between consumption and biodiesel production, as well as issues related to cost efficiency. To address these availability and cost concerns, the utilization of used cooking oil as a foundational material for biodiesel synthesis has been proposed. However, employing used cooking oil directly for biodiesel synthesis is generally deemed impractical, particularly for diesel engines featuring direct and indirect injection systems [2,3]. Consequently, the conversion of waste cooking oil into its constituent fatty acids becomes imperative for biodiesel production [4]. Nevertheless, this conversion step introduces a new set of challenges.

In used cooking oil, there is a substantial concentration of free fatty acid (FFA) or fatty acids, making esterification and transesterification through various catalytic reactions such as lipase-catalyzed, photo-catalyzed, alkaline-catalyzed, and acid-catalyzed processes the most suitable methods for converting used cooking oil [5,6,7]. In large-scale biodiesel production, the lipase-catalyzed transesterification method is not widely adopted due to its extended reaction time and lower cost efficiency when compared to acid and alkali-catalyzed reactions

http://doi.org/10.20473/jbiome.v1i2.51930

[8,9]. Previous studies have indicated the feasibility of biodiesel production using ZnO/SiO_2 photocatalysts in the esterification of free fatty acids (FFA) from *Jatropha curcas* crude oil [10]. Additionally, solar radiation can induce the conversion of FFA from waste cooking oil into methyl esters via a Cr/SiO_2 photocatalyst reaction [6]. This suggests that photocatalytic transesterification holds significant potential for biodiesel production. However, it's noteworthy that photocatalysis technology is primarily limited to laboratory settings and necessitates further development and research. Esterification and transesterification reactions typically involve alkaline catalysts such as NaOH/Zeolite and KOH [11,12]. Nonetheless, these reactions introduce a new set of challenges. This poses an issue because the typical biodiesel synthesis involves a transesterification reaction employing a basic catalyst, which results in catalyst deactivation.

Solid acid catalysts such as Nafion and Amberlyst are used to overcome this barrier. The product Nafion, the main subject of this study, is a fluoropolymer-copolymer resin produced by DuPont and is classified as a sulfonated tetrafluoroethylene compound [13]. Because it contains three extremely electronegative fluoride atoms that make protons easier to release, Nafion is noticeably acidic. At the moment, Nafion is used in two main forms: Nafion NR50, which is a resin, and Nafion SAC-13, which is a silica nanocomposite that incorporates Nafion NR50 to increase the surface area of the catalyst [14].

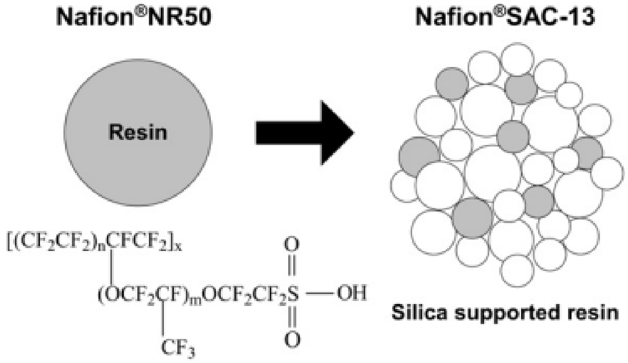

Fig 1. The Structure of Nafion NR50 and SAC-13

While there are two variations of Nafion, both follow the same reaction mechanism. Nevertheless, the in-depth quantum reaction mechanism of this catalyst has not been thoroughly explored despite its recognized effectiveness and selectivity in generating methyl ester and glycerol products [15].

Previous studies have delved into the transesterification of FFA with acid catalysts using the ab-initio method [16]. However, further investigations into Nafion catalysts and their mechanisms, particularly through density functional theory (DFT) studies, which explore system interactions and suggest that potent acid catalysts can effectively lower the Gibbs free energy of transesterification in biodiesel production [17], have been lacking. Augusto et al.

employed DFT to analyze the acid-catalyzed ethanolysis process of butyric acid monoacylglycerol and highlighted the crucial role of intrinsic hydrogen bonding in stabilizing tetrahedral intermediates when considering solvent effects [18]. Therefore, there is a need for the application of quantum chemical or computational methods with a specific theoretical approach. This study aims to precisely investigate the reaction mechanisms of FFA transesterification (simplified to mono esters in the form of methyl esters) and acetic acid esterification. The comparison will be made with the DFT method and the PM7 semi-empirical level of theory. The primary reaction mechanism and intermediates will be explored computationally based on calculated thermodynamic and kinetic data. These findings will offer a comprehensive understanding of the reaction mechanism and establish a theoretical foundation for biodiesel production from used cooking oil.

2. Materials and methods

The study involved an analysis of acetic acid esterification and FFA transesterification reactions, which were transformed into methyl esters. These investigations were conducted utilizing Gaussian 16 [19] and DFT, specifically employing the semi-empirical Parametric Method 7 (PM7) theory at the atomic level. PM7 was chosen because of its low computational cost and demonstrated superior accuracy for hydrogen-bonded complexes due to explicit corrections for such interactions [20]. To ensure the accuracy of the results, all molecular structures were subject to geometric optimization, both with and without the presence of the Nafion catalyst, with a requirement for achieving "Converged" outcomes across all parameters before identifying the transition state (TS). For simplification and acceleration of calculations, a 6-ring complex was chosen as the TS model. Validation of the TS was accomplished through the identification of a single imaginary frequency, coupled with the transformation from reactant/intermediate to intermediate/product. To enhance the precision of energy calculations, a single-point energy calculation was additionally conducted, employing the M062X level with the 6-31+g(d, p) basis set.

3. Results and discussion

Esterification and transesterification share comparable reaction mechanisms but involve distinct sets of reactants and yield different products. Esterification requires a carboxylic acid and an alcohol, resulting in the formation of an ester and water. On the other hand, transesterification involves an ester and an alcohol, leading to the generation of a new ester and a new alcohol. In this research, the esterification reaction was examined using acetic acid, while transesterification was studied using methyl acetate.

3.1. Acetic Acid Esterification

The reaction mechanism of acetic acid esterification with and without catalyst can be seen in the following figure 2.

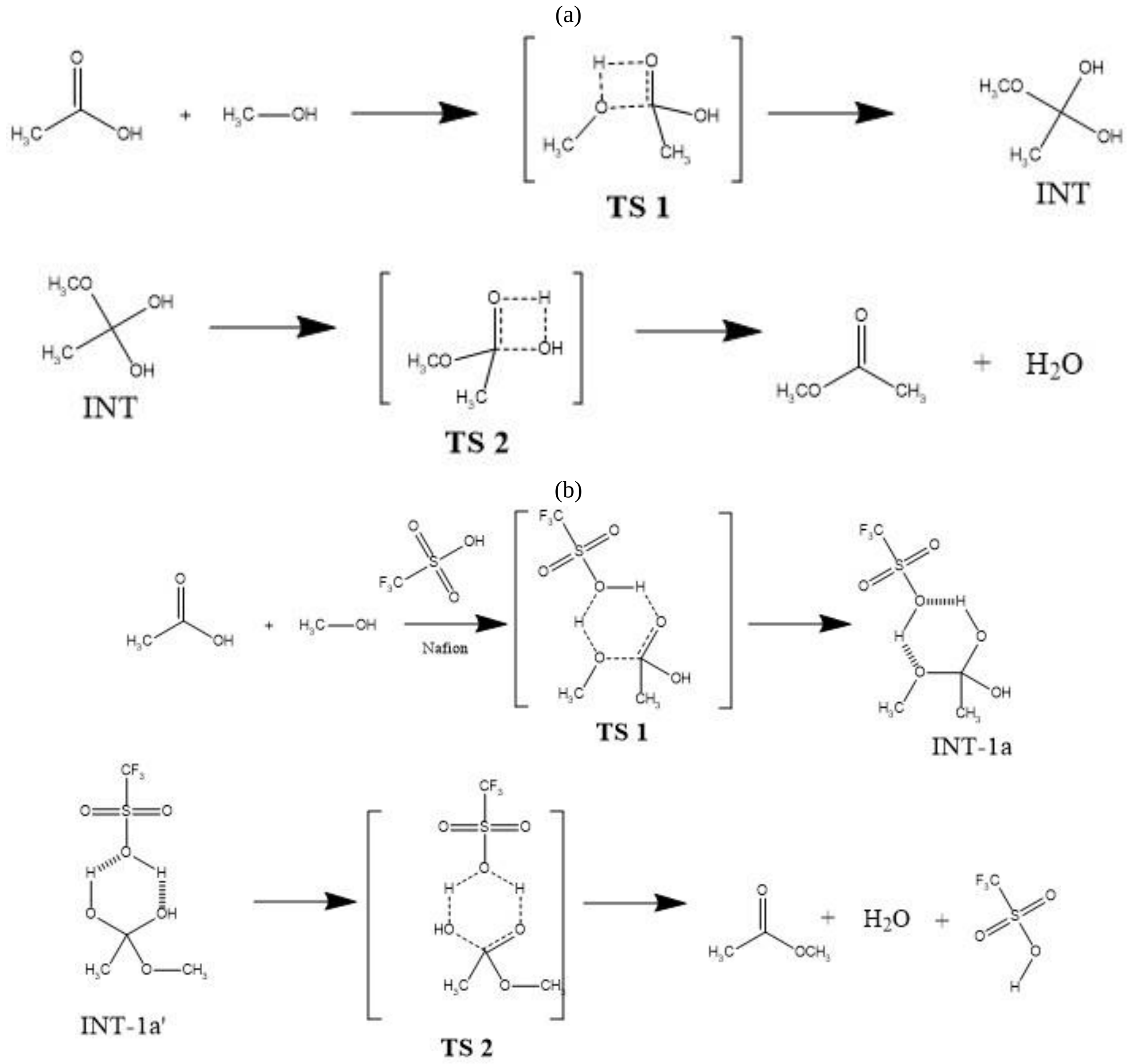

Fig 2. Esterification reaction of acetic acid without (a) and with (b) Nafion catalyst.

The esterification of acetic acid results in the production of methyl ester and water. In the absence of a catalyst, an initial 4-ring complex forms at TS1, producing an acetal as an intermediate. Subsequently, from this intermediate, TS2 emerges, also as a 4-ring complex, culminating in the production of the desired product.

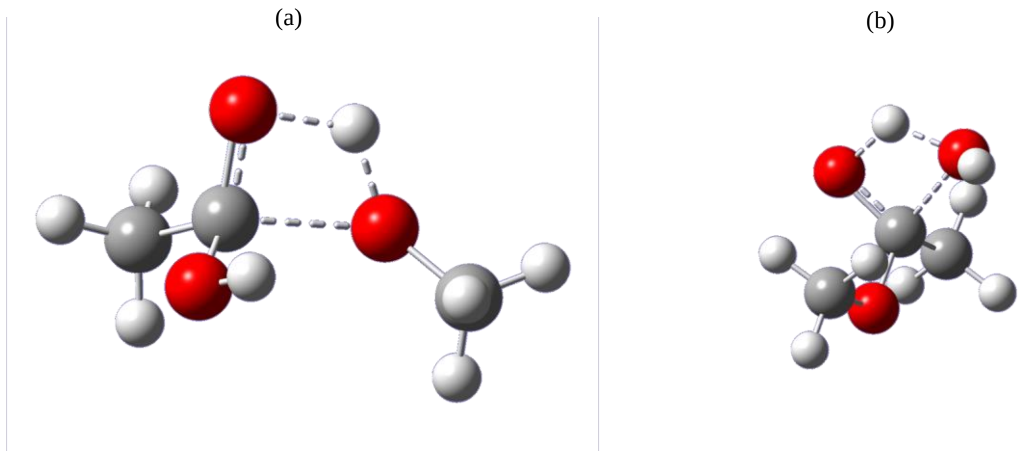

Fig 3. Structures of TS1 (a) and TS2 (b) from the reaction without catalyst.

In the presence of Nafion, its role involves assisting in the disruption of the double bond between carbon and oxygen within the carbonyl group. This is achieved through hydrogen bonding with two existing oxygen atoms, giving rise to a 6-ring complex at TS1 and the intermediate phase. The Nafion within the Nafion-intermediate complex then transitions to establish hydrogen bonds with another oxygen atom, ultimately yielding the final product in the form of methyl ester and water, along with the participation of Nafion.

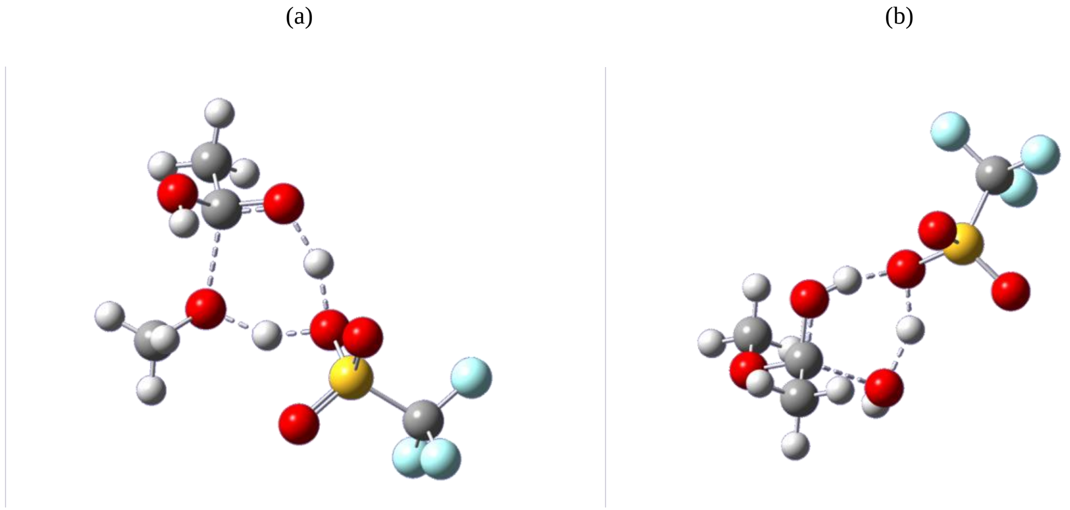

Fig 4. Structures of TS1 (a) and TS2 (b) from the reaction with Nafion catalyst.

To ensure the reliability of all transition states (TS) generated during the reaction, computational verification was conducted using the Intrinsic Reaction Coordinate (IRC) method, as TS structures are inherently unstable and challenging to isolate [21].

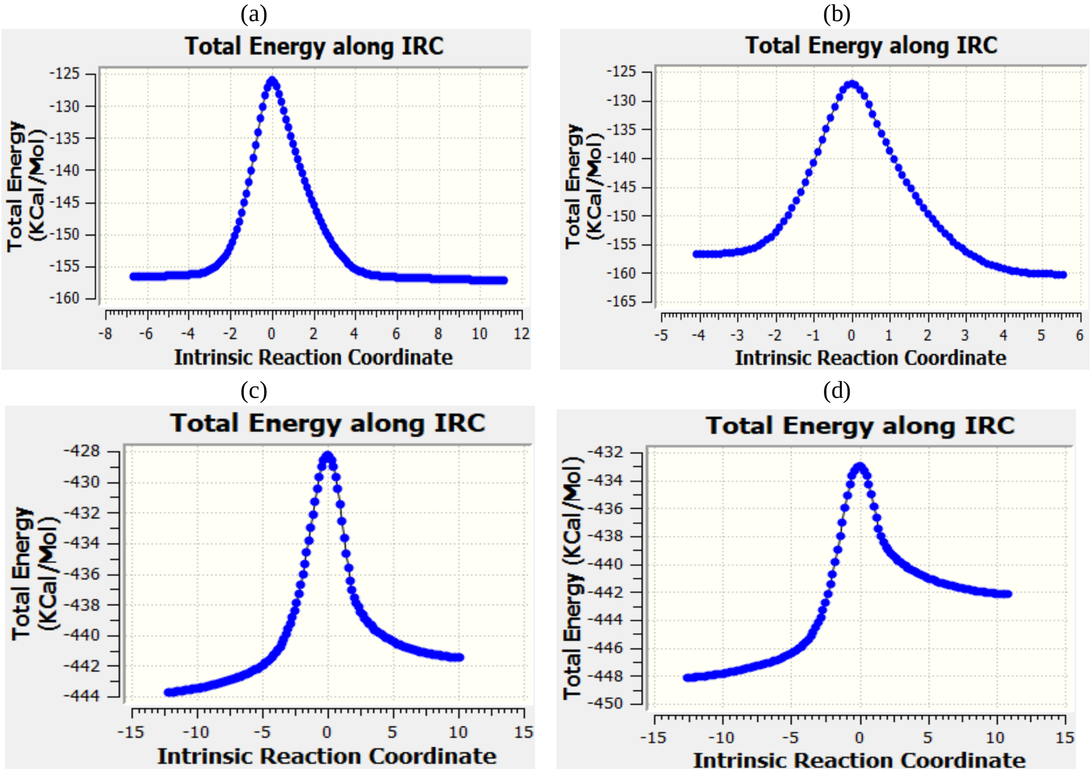
(a) (b) (c) (d)

Fig 5. IRC graph of TS Esterification. Without catalyst, TS1 (a) and TS2 (b). With Nafion catalyst, TS1 (c) and TS2 (d).

The obtained results indicate that the transition state (TS) energy in the presence of the Nafion catalyst exhibits a lower overall energy when contrasted with the TS in the absence of a catalyst. This difference can be attributed to the catalyst's role in reducing the overall activation energy required for the reaction.

3.2. Methyl Ester Transesterification

In contrast to esterification, transesterification of methyl ester compounds is reversible, with only the exchange of methyl functional groups from methanol to methyl ester and vice versa. The mechanism of the methyl ester transesterification reaction is depicted in the following figure.

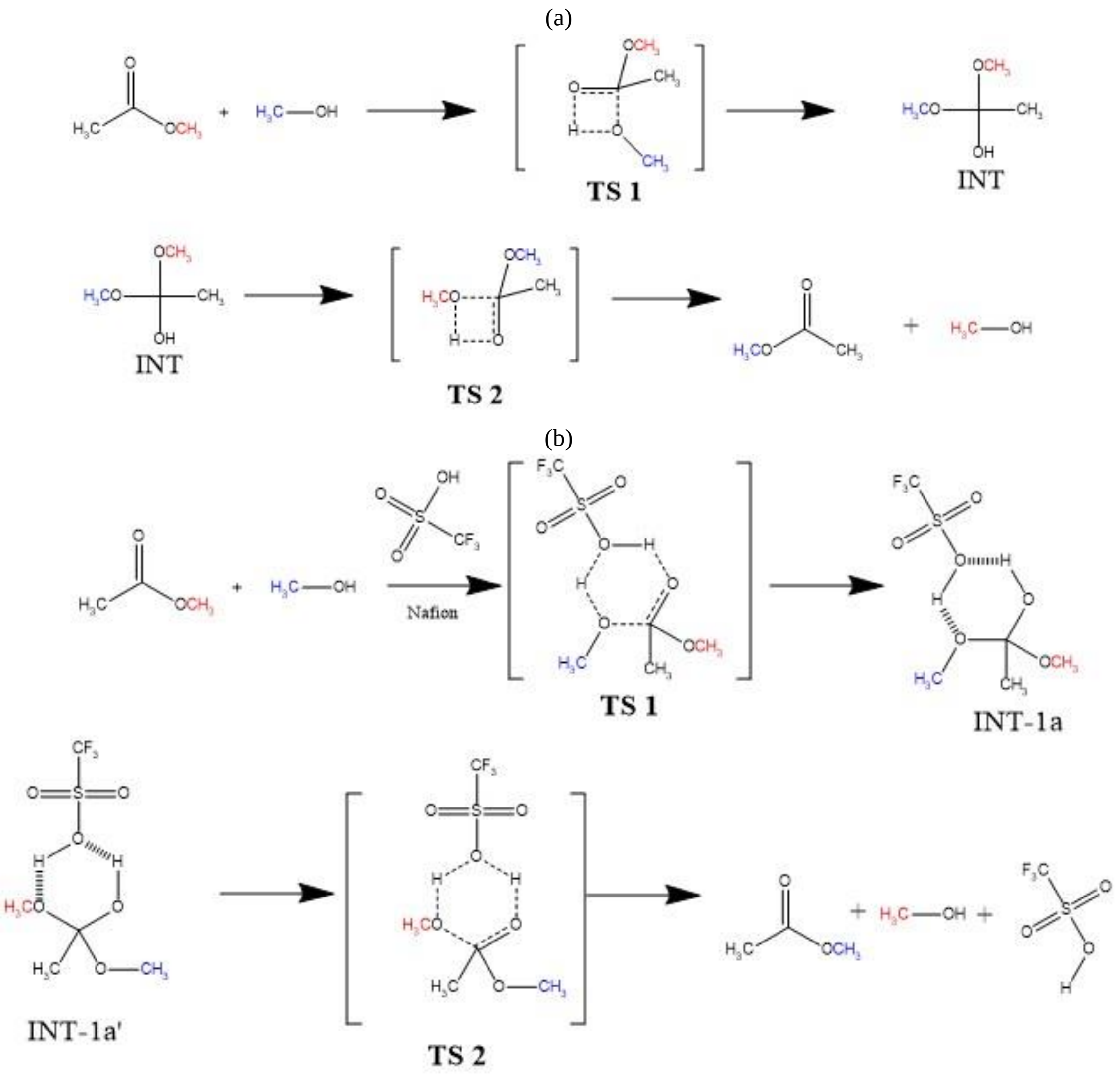

Fig 6. Transesterification reaction of methyl esters without (a) and with (b) Nafion catalyst.

In general, the mechanism for the transesterification reaction closely resembles that of esterification, including cases with and without the Nafion catalyst. As depicted in Figure 7, it is evident that there is an exchange of two methyl groups, where methyl ester molecules (red) swap their methyl groups with those from methanol (blue). Similar to esterification, in the absence of a catalyst, the reaction leads to the formation of a transition state (TS) featuring a 4-

ring complex. Conversely, in the presence of Nafion, a TS characterized by a 6-ring complex is formed. Both scenarios exhibit reversible reactions, as the reactants are regenerated, with the primary distinction being the exchange of methyl groups.

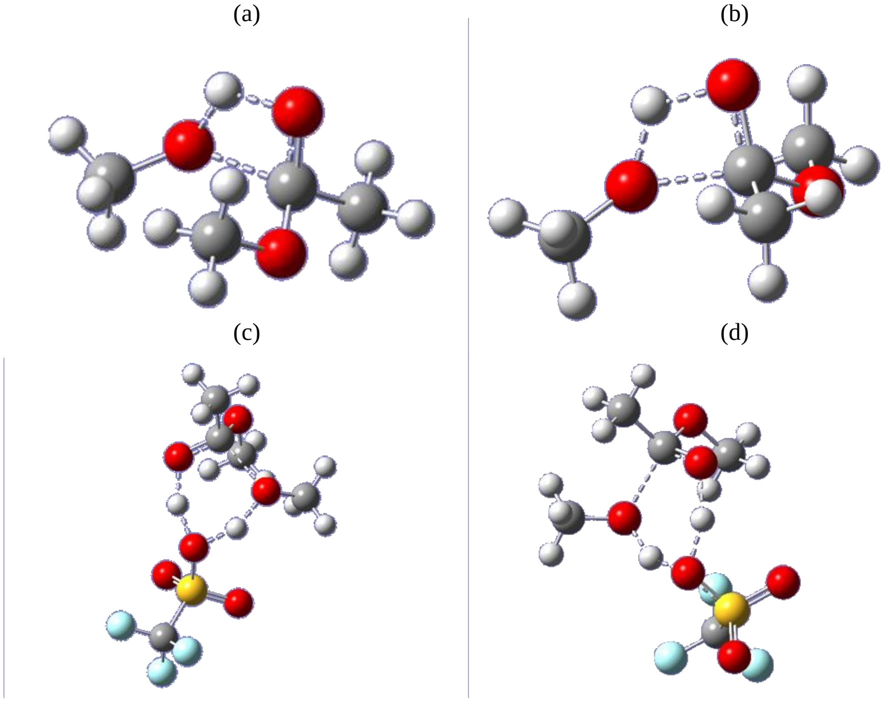
(a) (b)
(c) (d)

Fig 7. TS transesterification without catalyst (a) TS1 and (b) TS2; (c) TS1 and (d) TS2 with nafion

The TS of this reaction has also been verified and analyzed using IRC by connecting the reactants and products with the TS.

(a) (b)

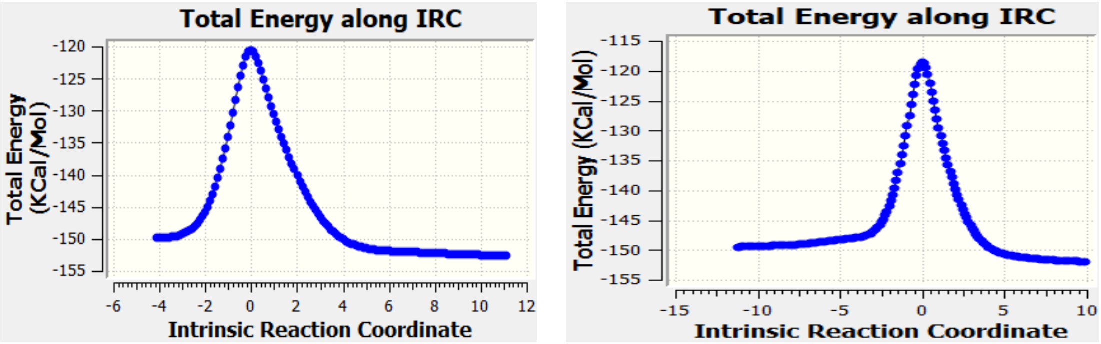

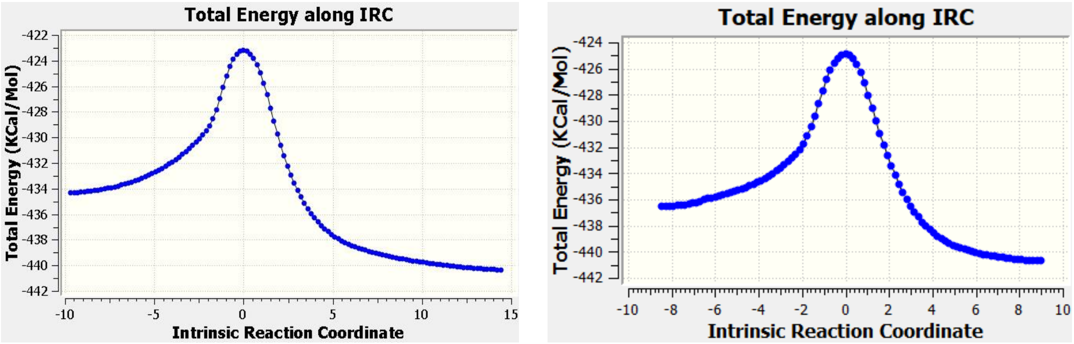
(c) (d)

Fig 8. IRC graph of TS Transesterification. Without catalyst, TS1 (a) and TS2 (b). With Nafion catalyst, TS1 (c) and TS2 (d).

Based on the results found, the energy of TS with the Nafion catalyst has a lower energy than without the catalyst. This is also the same compared to the results obtained in the esterification reaction.

3.3. Reaction Energetics

Initially, the energy aspects of the esterification reaction were examined. This involved assessing data derived from the optimization outcomes and frequency structure of reactants, transition states (TS), intermediates, and products, ensuring that all calculations had reached a state of "Converged" results. The energy data and the reaction coordinate diagram were subsequently acquired in the following manner.

Table 1. Relative Gibbs energy of each species in acetic acid esterification reaction (1 atm)

Specs	**Acetic Acid Esterification Energies (kJ/mol)**	
	Without Catalyst	**With Catalyst**
Reactants (Acetic Acid + Methanol)	0	0
Transition State 1 (TS1)	164,4902	99,7453
Intermediate	40,5560	40,5560
Transition State 2 (TS2)	159,6960	99,7453
Products (Methyl Ester + Water)	-17,8627	-17,8627

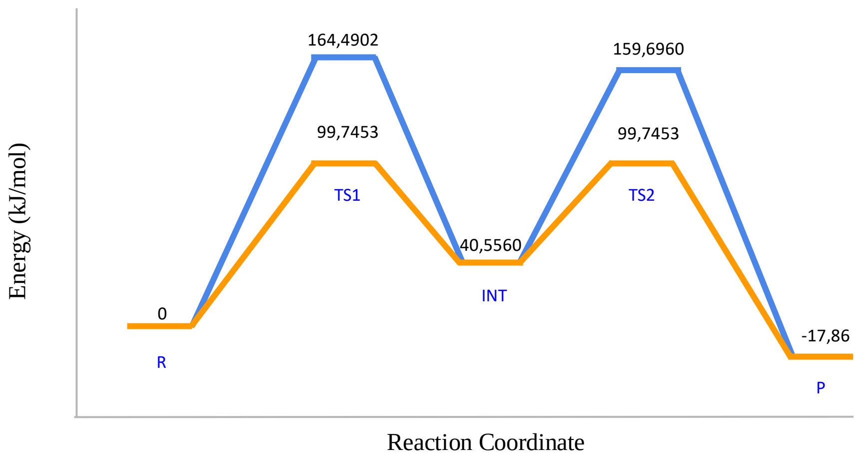

Table 2. Relative ΔG value of acetic acid esterification reaction (1 atm)

ΔG Types	**ΔG Values (kJ/mol)**	
	Without Catalyst	**With Catalyst**
ΔG1	164,4902	99,7453
ΔG2	159,6960	99,7453

Fig 9. Reaction diagram of acetic acid esterification (blue) without catalyst and (orange) with Nafion.

The diagram illustrates the position and energy profile of the acetic acid esterification reaction. It's evident from the diagram that the presence of the Nafion catalyst effectively reduces the activation energy required for the reaction. This observation is supported when examining the ΔG (Gibbs free energy) value, which shows that the presence of the Nafion catalyst results in lower energy requirements. Specifically, the ΔG value for activation in both stages with the Nafion catalyst is lower compared to the reaction without the catalyst. Both reactions share the same rate-determining stage (RDS), which is the formation of TS1. This occurs because the ΔG1 value for activation in both stages is greater than the ΔG2 value for activation to form TS2.

A similar pattern is observed when comparing the enthalpy values (under conditions of 1 M and 298 K) in TS. The obtained enthalpy data corroborate the findings of reduced energy requirements.

Table 3. TS Enthalpy energy of acetic acid esterification reaction (1M)

ΔH Types	**ΔH Values (kJ/mol)**	
	Without Catalyst	**With Catalyst**
TS1	$-4,2497 \times 10^{-4}$	$-7,3416 \times 10^{-5}$
TS2	$-4,1674 \times 10^{-4}$	$-7,2344 \times 10^{-5}$

This data further reinforces the notion that the presence of a catalyst reduces the activation energy, confirming that the esterification reaction is exothermic. The analysis of reaction energetics for the transesterification reaction yielded outcomes akin to those observed in the esterification reaction. This similarity arises from the fundamental similarity in the reaction mechanisms. The subsequent data and graphs provide a clearer picture of these results.

Table 4. Relative Gibbs energy of each species in methyl ester transesterification reaction (1 atm, 298°K)

Specs	**Acetic Acid Esterification Energies (kJ/mol)**	
	Without Catalyst	**With Catalyst**
Reactants (Methyl Ester + Methanol)	0	0
Transition State 1 (TS1)	196,7707	101,4650
Intermediate	51,3889	51,3889
Transition State 2 (TS2)	169,1872	96,0539
Products (Methyl Ester + Water)	0	0

Table 5. Relative ΔG value of methyl esterification reaction (1 atm, 298°K)

ΔG Types	**ΔG Values (kJ/mol)**	
	Without Catalyst	**With Catalyst**
ΔG1	196,7707	101,4650
ΔG2	169,1872	96,0539

Fig 10. Diagram of methyl ester transesterification reaction (blue) without catalyst and (orange) with Nafion.

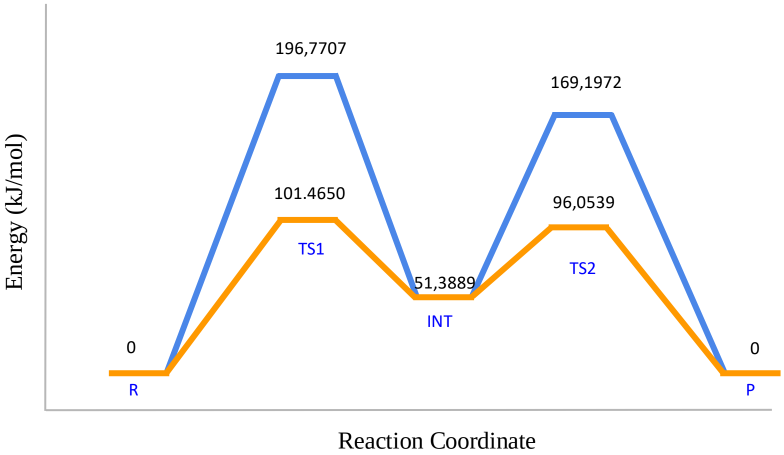

These results also elucidate that the presence of the catalyst reduces the activation energy necessary for the transesterification reaction in comparison to its absence. However, as this reaction yields the same products as the reactants, the ΔG^0 value does not exist. Consequently, both rate-determining stages (RDS) are primarily attributed to activation ΔG^1 because its ΔG value surpasses the activation ΔG^2 value. Presented below are the enthalpy values for the transition state (TS) in the methyl ester transesterification reaction.

Table 6. TS enthalpy energy in methyl ester transesterification reaction (1M)

ΔH Types	**ΔH Values (kJ/mol)**	
	Without Catalyst	**With Catalyst**
TS1	-8,78 x 10^{-4}	-7,83 x 10^{-4}
TS2	-7,12 x 10^{-4}	-7,72 x 10^{-4}

In this study, the analysis of esterification and transesterification reactions also considers the calculation of reaction rate constants using the principles of transition state theory. This analysis is conducted through the utilization of the Eyring formula and the Wigner method. The objective is to explain why the presence of a catalyst can reduce the necessary activation energy. This methodology involves two equations as follows:

$$k_{TST} = \sigma K v\, e^{\frac{\Delta G^{\ddagger}}{RT}} \tag{1}$$

$$k = 1 + \frac{1}{24}\left(\frac{hcv^{\ddagger}}{k_B T}\right)^2 \tag{2}$$

Equation (1), necessitates obtaining imaginary vibrational data derived from the transition state (TS), while equation (2), requires the value of k (quantum breakthrough) that has been determined, along with the Gibbs value from the TS. To ensure accurate calculations, the Gibbs value initially must be converted from a state of 1 atm (ideal gas) to 1 M under realistic conditions, which can be achieved using the following equation [22].

$$\Delta G^{\ddagger,1M} = \Delta G^{\ddagger,1atm} - RT\ln(24{,}5) \tag{3}$$

The initial Gibbs energy data is converted using equation (3) to obtain values applicable in the 1 M state. These data are subsequently used in equation (1) along with the imaginary frequency data obtained from each transition state.

Table 7. Imaginary frequency TS of esterification and transesterification reactions.

TS	Esterification (m^{-1})		Transesterification (m^{-1})	
	Without Catalyst	**With Catalyst**	**Without Catalyst**	**With Catalyst**
TS1	-133482	-54850	-134849	-46266
TS2	-137969	-46982	-133689	-42042

From the imaginary frequency data of each TS and also the Gibbs energy values of all TS, it is substituted into equation (1) and then (2). The following results were obtained.

Table 8. K and K TST values of each TS of esterification and transesterification reactions

TS	Esterification		Transesterification	
	Without Catalyst	**With Catalyst**	**Without Catalyst**	**With Catalyst**
K TS1	2,73	1,29	2,76	1,20
K TS2	2,85	1,21	2,73	1,17
K TST TS1	$3{,}89 \times 10^5$	$7{,}38 \times 10^5$	$4{,}04 \times 10^5$	$5{,}82 \times 10^5$
K TST TS2	$4{,}12 \times 10^5$	$5{,}84 \times 10^5$	$3{,}84 \times 10^5$	$5{,}02 \times 10^5$

The results of the K and K TST calculations indicate that when a catalyst is present, there is a noticeable quantum enhancement in the reaction rate. This enhancement leads to a faster progression of the reaction, as evidenced by a smaller K value compared to when no catalyst is present. Additionally, there is a substantial impact on TS1, and it occurs more rapidly in the presence of the catalyst, as indicated by a higher K TST value with the catalyst compared to without it.

Quantum breakthrough demonstrates that in the presence of a catalyst, the reaction requires less activation energy compared to when it proceeds without a catalyst. This phenomenon elucidates why the activation energy decreases when a catalyst is involved [23]. According to the calculations, the K value is strongly influenced by the imaginary frequency, and the presence of the catalyst shortens this imaginary frequency, making it easier for molecules to undergo reaction.

4. Conclusions

Based on the conducted experiments, it can be concluded that computational evidence affirms the ability of the Nafion catalyst to accelerate both esterification and transesterification reactions through the formation of a 6-ring complex at the transition state (TS). In both reactions, whether with or without the Nafion catalyst, the rate-determining step (RDS) is associated with the activation energy required to form TS1, as it exhibits the highest activation energy compared to the second activation energy. Through the calculation of quantum breakthrough and reaction rate constants, it is substantiated that the presence of Nafion catalysts leads to a quantum breakthrough, explaining the reduction in activation energy and confirming the acceleration of the reaction rate.

Acknowledgments

The authors would like to express their gratitude to the Department of Chemistry at the Faculty of Science and Technology, Universitas Airlangga, for granting permission to conduct molecular mechanics research on esterification and transesterification with and without Nafion catalyst. Your support and cooperation were instrumental in the successful completion of this study.

References

[1] Hoekman, S.K., Broch, A., Robbins, C., Ceniceros, E., and Natarajan, M. (2012). Review of biodiesel composition, properties, and specifications, Renewable and Sustainable Energy Reviews, 16(1), 143-169, ISSN 1364-0321.

[2] Muniyappa, P. R., Brammer, S. C., and Naureddini, H. 1996. Improved conversion of plant oils and animal fats into biodiesel and co-products. Bioresource Technology. 56(1), 19-24.

[3] Ramadhas, A., Jayaraj, S., & Muraleedharan, C. (2005). Biodiesel production from high FFA rubber seed oil. Fuel, 84(4), 335–340.

[4] Demirbas, A. (2009). Progress and recent trends in biodiesel fuels. Energy Conversion and Management, 50 (1), 14-34.

[5] Al-Zuhair, S. (2005), Production of Biodiesel by Lipase-Catalyzed Transesterification of Vegetable Oils: A Kinetics Study. Biotechnol Progress, 21: 1442-1448.

[6] Corro, G., Sanchez, N., Pal, U., Cebada, S., and Fierro, J. L. G. (2017). Solar-irradiation-driven biodiesel production using Cr/SiO2 photo catalyst exploiting cooperative interaction between Cr6+ and Cr3+ moieties. Applied Catalysis B: Environmental, 203, 43-52.

[7] Leung, D. Y. C., Wu, X., and Leung, M. K. H. (2010). A review on biodiesel production using catalyzed transesterification. Applied Energy, 87(4), 1083-1095.

[8] Meher, L.C., Sagar, D.V., and Naik, S.N. (2006). Technical Aspects of Biodiesel Production by Transesterification—A review, Renewable and Sustainable Energy Reviews 10(3), 248-268.

[9] Zhang, Y., Dube, M.A., McLean, D.D., and Kates, M. (2003). Biodiesel production from waste cooking oil: 2. Economic assessment and sensitivity analysis, 90(3), 229-240.

[10] Corro, G., Pal, U., and Tellez, N. (2013). Biodiesel production from Jatropha curcas crude oil using ZnO/SiO2 photocatalyst for free fatty acids esterification. Applied Catalysis B: Environmental, 129, 39-47.

[11] Zhang, L., Sheng, B., Xin, Z., Liu, Q., & Sun, S. (2010). Kinetics of transesterification of palm oil and dimethyl carbonate for biodiesel production at the catalysis of a heterogeneous base catalyst. Bioresource Technology, 101(21), 8144–8150.

[12] Kurniasih, E., & Pardi, P. (2020). Transesterification Condition of Crude Palm Oil to Biodiesel Using Solid Catalyst Zeolite/NaOH. In IOP Conference Series: Materials Science and Engineering (Vol. 854, No. 1, p. 012003). IOP Publishing.

[13] Church, Steven (2006). Del. firm installs fuel cell. The News Journal. p. B7.

[14] López, D. E., Goodwin Jr, J. G., & Bruce, D. A. (2007). Transesterification of triacetin with methanol on Nafion® acid resins. Journal of Catalysis, 245(2), 381-391.

[15] Lopez, D. E., Goodwin Jr, J. G., Bruce, D. A., & Lotero, E. (2005). Transesterification of triacetin with methanol on solid acid and base catalysts. Applied Catalysis A: General, 295(2), 97-105.

[16] Zaramello, L., Kuhnen, C. A., Dall'Oglio, E. L., & de Sousa Jr, P. T. (2012). DFT study of gas phase acid-catalyzed ethanolysis of butyric acid triglyceride. Fuel, 94, 473-479.

[17] Muniz, E.C., Caldas, B.S., Nunes, C.S., Souza, P.R., Rosa, F.A., Visentainer, J.V., and Junior, O.O.S. (2016). Applied Catalysis B: Environmental, 181, 289-297.

[18] da Silva, A.C.H., Dall'Oglio, E.L., de Sousa Jr., P.T., da Silva, S.C., and Kuhnen, C.A. (2013). DFT study of the acid-catalyzed ethanolysis of butyric acid monoglyceride: Solvent effects. Fuel, 119, 1-5.

[19] M. J. Frisch, G. W. Trucks, H. B. Schlegel, G. E. Scuseria, M. A. Robb, J. R. Cheeseman, G. Scalmani, V. Barone, G. A. Petersson, H. Nakatsuji, X. Li, M. Caricato, A. V. Marenich, J. Bloino, B. G. Janesko, R. Gomperts, B. Mennucci, H. P. Hratchian, J. V. Ortiz, A. F. Izmaylov, J. L. Sonnenberg, D. Williams-Young, F. Ding, F. Lipparini, F. Egidi, J. Goings, B. Peng, and A. Petrone. (2016). Gaussian 16, Revision A.03; Gaussian, Inc.: Wallingford CT.

[20] Alzahrani, K. A. R. M. G., Alshahrani, A. R. M., and Alharthi, M. A. A. (2015). Accuracy issues involved in modeling in vivo protein structures using PM7. Proteins: Structure, Function, and Bioinformatics, 83, 1427–1435.

[21] Schlegel, H.B. (2003). Exploring potential energy surfaces for chemical reactions: An overview of some practical methods. Computational Chemistry, 3(2), 214-218.

[22] Vásquez-Espinal, A., Yañez, O., Osorio, E., Areche, C., García-Beltrán, O., Ruiz, L. M., and Tiznado, W. (2019). Theoretical study of the antioxidant activity of quercetin oxidation products. Frontiers in Chemistry, 7, 818.

[23] Ghosh, N., Kerns, S. J., and Laino, T. (2014). Eliminating Imaginary Vibrational Frequencies in Quantum Mechanical/Molecular Mechanical Calculations of Enzyme Catalysis. Journal of Chemical Information and Modeling, 54(8), 2334–2340.